

Fast 1D NMR imaging of clay sedimentation using a multi-slice stepper motor method

Hol, Nick J.; Pel, Leo; Kurvers, Martijn; Chassagne, Claire

DOI

[10.1007/s00348-024-03937-3](https://doi.org/10.1007/s00348-024-03937-3)

Publication date

2024

Document Version

Final published version

Published in

Experiments in Fluids

Citation (APA)

Hol, N. J., Pel, L., Kurvers, M., & Chassagne, C. (2024). Fast 1D NMR imaging of clay sedimentation using a multi-slice stepper motor method. *Experiments in Fluids*, 66(1), Article 9. <https://doi.org/10.1007/s00348-024-03937-3>

Important note

To cite this publication, please use the final published version (if applicable). Please check the document version above.

Copyright

Other than for strictly personal use, it is not permitted to download, forward or distribute the text or part of it, without the consent of the author(s) and/or copyright holder(s), unless the work is under an open content license such as Creative Commons.

Takedown policy

Please contact us and provide details if you believe this document breaches copyrights. We will remove access to the work immediately and investigate your claim.

Green Open Access added to TU Delft Institutional Repository

'You share, we take care!' - Taverne project

<https://www.openaccess.nl/en/you-share-we-take-care>

Otherwise as indicated in the copyright section: the publisher is the copyright holder of this work and the author uses the Dutch legislation to make this work public.



Fast 1D NMR imaging of clay sedimentation using a multi-slice stepper motor method

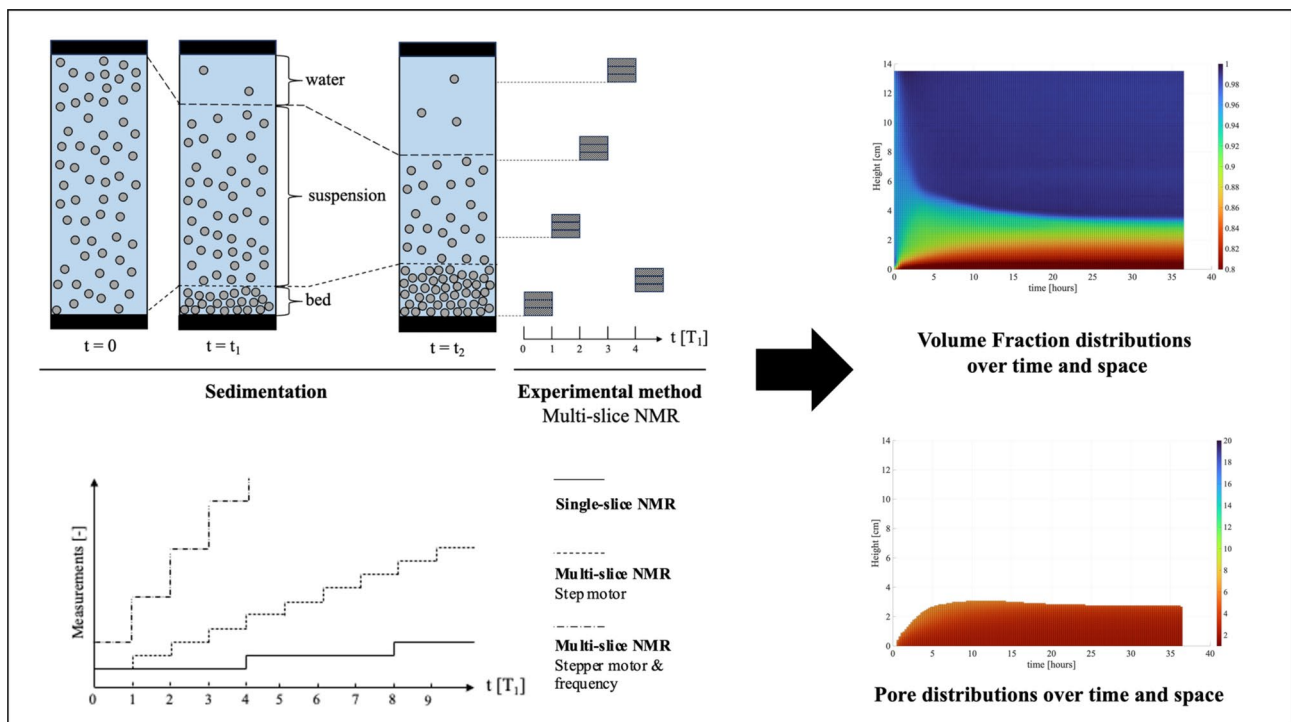
Nick J. Hol¹ · Leo Pel¹ · Martijn Kurvers¹ · Claire Chassagne²

Received: 19 August 2024 / Revised: 17 October 2024 / Accepted: 6 December 2024
© The Author(s), under exclusive licence to Springer-Verlag GmbH Germany, part of Springer Nature 2024

Abstract

This study introduces a fast 1D nuclear magnetic resonance (NMR) imaging method based on multi-slice imaging with a stepper motor to study sedimentation dynamics of clayey soils. Traditional NMR is limited by long acquisition times due to water's T_1 relaxation time. Our approach combines multi-slice imaging with a stepper motor and frequency-based selection, reducing measurement time while maintaining sub-millimeter resolution, at the same time overcoming the limitations by the slow relaxation of water. This nondestructive method provides detailed insights into the sedimentation and consolidation of suspensions, including pore size distribution and density profiles within a single measurement. The technique is demonstrated with kaolinite clay suspensions, highlighting the technique's ability to capture the dynamics of gravity-driven systems rapidly and accurately, even for fast-sedimenting soils such as kaolinite in the first hours of sedimentation. This advancement is valuable for geotechnical and environmental applications where understanding sedimentation is crucial.

Graphical abstract



Extended author information available on the last page of the article

1 Introduction

Yearly, over 200 million cubic meters of fine-grained soil is dredged Europe-wide. This soil, consisting mostly of nano- and micron-sized clay particles, is usually seen as a waste source with low economic value. Research on this fine-grained clay sludge is currently ongoing to check whether this material can be used as a cost-effective construction material for the application on dikes and embankments, among others. To make these clay sludges suitable for this purpose, their mechanical properties must be adapted such that they comply with safety regulations.

An important step in this process is the understanding of the sedimentation and consolidation properties of clay sludges over time. The sedimentation and consolidation of thick clay suspensions (sludges) is a complex multi-stage process with varying time scales in the initial hindered settling and later consolidation phases, ranging from minutes to days. This process of clay sludge transforming into a three phases system, consisting of a concentrated sediment bed, a suspension and a nearly particle-free water layer is given schematically in Fig. 1. Here an initially homogenous suspension of fine-grained clay particles in water settles under the influence of gravity. Over time, the height of the suspension layer decreases, forming a consolidated sediment bed below the suspension layer while a clear water layer above the suspension layer grows. At the so-called gelling point (or gel time), the suspension layer disappears entirely, and a nearly particle-free water layer and consolidated particle bed remain.

From recording the interfaces between the different phases and the density evolution of the sludge over time as

function of height, the hydraulic conductivity and effective stress of the clay sludge can be derived to verify numerical models and thereby get a better understanding of the relation between sludge composition and its settling/consolidation properties (Been and Sills 1981; Merckelbach and Kranenburg 2004). This composition is a function of different parameters, such as particle size distributions, clay type and concentration, presence of organic matter, pH, temperature, and salinity of the suspension which also directly affect the sedimentation and consolidation properties (Chassagne 2021; Imai 1981; Naghipour et al. 2014; Xuekui and Qingqing 2021). A high temporal and spatial resolution is essential in order to be able to accurately differentiate the various stages within the sedimentation and consolidation process.

As clay suspensions are a non-transparent media, inspection by nondestructive camera systems or optical-based densimeters only give limited information of the time-dependent sedimentation and consolidation profiles (Sutherland et al. 2015). Pore pressure transducers (PPTs) can be added to supply additional information about pore size distributions and pressures, however the spatial resolution of these PPT's is limited. Computed tomography (CT) has been used as a nondestructive method to investigate clay sedimentation in which 2D/3D images giving direct access to density profiles (Fouinat et al. 2017; Reilly et al. 2017).

In this study, nuclear magnetic resonance (NMR) is used as it has the option not to only give direct access to the moisture content and thereby to the sludge density but could also provide direct information on the pore size distribution in the particle bed and even on diffusivity, something that cannot be assessed by CT scans (Elsayed et al. 2023; Fleury et al. 2011; Komoroski 1993; Valckenborg

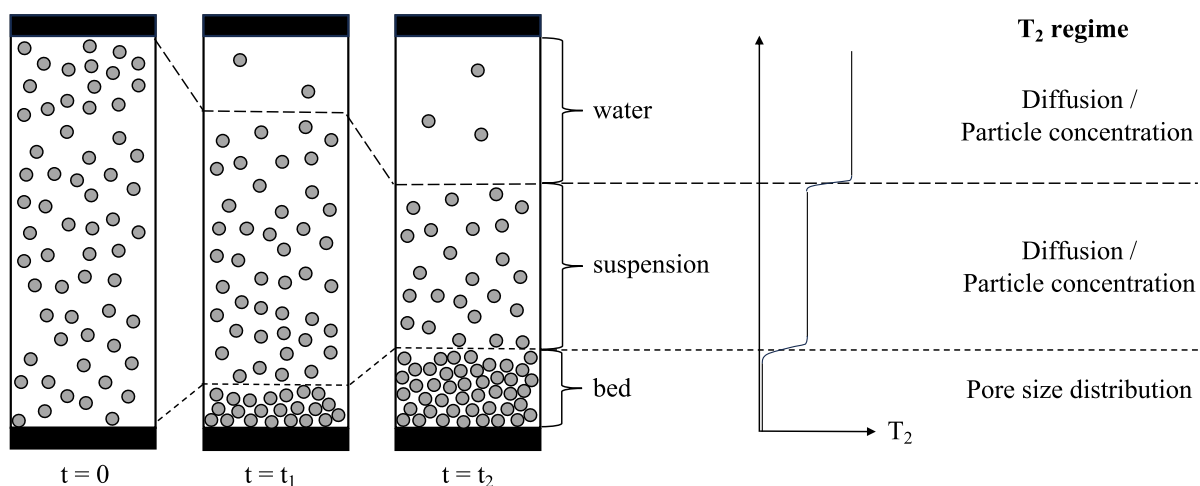


Fig. 1 A schematic representation of the sedimentation and consolidation process of clay suspensions. Indicated are the settling regimes as can be identified, i.e., a settled bed of particles, a suspension, and

a clear water layer. On the right the expected T_2 time of measured nuclear magnetic resonance signal with the associated T_2 regimes is indicated

et al. 2001a, b). While NMR offers advantages over other methods, the measurement speed of NMR imaging is limited by the relaxation time. To overcome this limitation, a multi-slice NMR imaging protocol is adapted that makes use of a stepper motor to effectively decrease the measurement time. Moreover, by combining the stepper motor method with frequency-based selection we decreased the acquisition time even further.

This technique is suitable for use in small-scale 1D NMR systems, comprising of electromagnets that generate low static fields (0.78 T), which have low gradients (± 0.1 T/m) and small coils (on the order tens of millimeters), distinguishing the technique from other more complicated stepper-based NMR methods used for sample alignment as opposed multi-slice imaging (Kresse et al. 2019). This technique improves the spatial and temporal resolution of acquired volume fraction and pore size distribution within samples. Here, a distinction is made between general, large (medical) magnetic resonance imaging (MRI) systems and small-scale NMR systems used in this research. While the smaller (1D) NMR machines can only measure samples with small cross sections (on the order of centimeters), they are able to measure these samples for hours, days or weeks on end giving comprehensive information on sedimentation characteristics and as a result are also more cost-effective.

Firstly, the NMR technique will be discussed and the multi-slice method using the stepper motor is proposed, after which an application of the NMR technique will be discussed on the sedimentation of a kaolinite clay suspension, showing that this NMR technique is suitable for analyzing gravity-driven systems, without being affected by the movement of the stepper motor.

2 Volume fraction and pore size profiles via NMR

2.1 Basic NMR principles

NMR is a nondestructive technique used to probe the internal structure of objects, such as suspensions, by utilizing the magnetic properties of atomic nuclei. The method is based on the principle that certain nuclei, such as hydrogen in water molecules, possess a magnetic moment. When an external magnetic field is applied to align these magnetic moments they can be manipulated by external radio frequency (RF) field, generating a signal from which information can be retrieved. For a basic introduction on NMR, the reader is referred to 'The Basics Of NMR' by Hornak (1996).

Most nuclei have a magnetic dipole moment because of their spin-angular momentum. The NMR Larmor frequency of a specific nucleus is given by:

$$f = \gamma B_0 \quad (1)$$

where f is the frequency, γ is the gyromagnetic ratio (42.58 MHz/T for ^1H) and B_0 is the applied magnetic field. The gyromagnetic ratio is dependent on the type of nucleus. NMR can therefore be made sensitive to only a particular type of nucleus, e.g., to hydrogen and thereby to water. The orientation of a magnetic dipole moment of nuclei in a sample can be manipulated by making use of pulsed RF fields at the Larmor frequency. The signal one retrieves in a pulsed NMR spin-echo or Carr–Purcell–Meiboom–Gill (CPMG) experiment is given by (Carr and Purcell 1954; Meiboom and Gill 1958):

$$S = k\rho_H \left(1 - e^{-\frac{TR}{T_1}}\right) e^{-\frac{TE}{T_2}}. \quad (2)$$

Here S is the retrieved signal, k is a proportionality constant which is 1 for hydrogen, ρ_H is the density of the proton spins in the sample, T_1 is the spin–lattice relaxation time and T_2 is the spin–spin relaxation time. The repetition time TR is a parameter that specifies the repetition time of the total pulse sequence, thus how frequently we are able to repeat an NMR measurement. The echo time TE is the time between the excitation RF pulse and the peak of the first spin-echo formed in the CPMG sequence, or more generally, between successive echoes in the CPMG echo train. Both TR and TE are graphically represented in the CPMG sequence in Fig. 2.

As seen from Eq. (2), the signal from the excited nuclei decays according to two distinct relaxation mechanisms. The spin–lattice relaxation T_1 is caused due to interactions between spins and their environment, whereas the spin–spin relaxation T_2 is due to interaction by the spins themselves.

In general, to neglect the T_1 contribution (we are only interested in effects caused by the T_2 relaxation) to the signal the repetition time is chosen as $TR > 4T_1$. Consequently, the repetition time of an NMR experiment is dominated by T_1 , and hence, the longest T_1 will dominate the total measurement time of a profile. Therefore, in our sedimentation experiment the repetition time is dominated by diffuse part where the T_1 relaxation of water is in the order of 3 s. Hence a single-slice spin-echo experiment takes in the order of 12 s and acquiring a total moisture profile of n -points will take n times 12 s.

2.2 Relaxation and pores size

Consider a cylindrical sample filled with a water-based clay suspension, which has an excited slice of volume V at height z , as given schematically in Fig. 3. Since the NMR signal is directly related to the proton density as given by Eq. (2), one can determine the volume fraction of water and clay in a slice from the NMR signal. In a two-component kaolinite

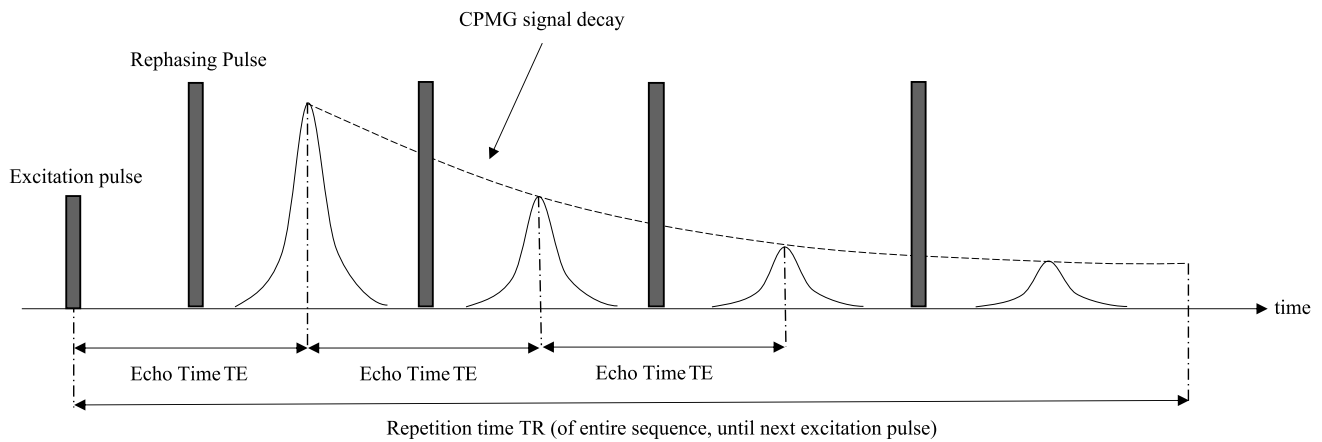


Fig. 2 Schematic representation of an NMR CPMG sequence with four echoes. First, an excitation pulse is applied. After a rephasing pulse (applied at time $TE/2$), an echo is observed. The time between

the excitation pulse and the first echo is given by the echo time. The repetition time TR is specified as the time between two entire CPMG sequences, i.e., the time between two successive NMR measurement

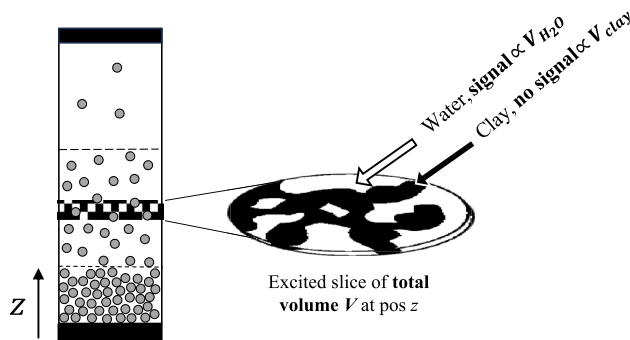


Fig. 3 Schematic representation of a sample with an excited slice at position z of total volume V , with a mix of kaolinite clay and water. Clay volumes do not contribute to signal, i.e., only signal is obtained from the free water

clay-water suspension, there are contributions to the hydrogen-based NMR signal from both the H nuclei enclosed within the OH- groups of suspended kaolinite particles, and the H nuclei from the water molecules. However, the T_2 relaxation of these clay-based OH- groups is so short (order 10^{-4} s) that with properly chosen spin-echo time TE no-signal contribution is obtained. Hence, the signal obtained is purely from the free water in the sample. Therefore, the volume fraction of clay in a sample is:

$$\phi_{\text{kaol}}(z) = 1 - \phi_{\text{water}}(z) = 1 - \frac{V_{\text{H}_2\text{O}}(z)}{V} = 1 - \frac{S_{t=0}(z)}{S_{\text{ref H}_2\text{O}, t=0}} \tag{3}$$

Here $\phi_{\text{water}}(z)$ is the water volume fraction at height z and $S_{\text{ref H}_2\text{O}, t=0}$ a reference signal of a volume slice containing only water molecules ($V_{\text{H}_2\text{O}} = V$).

In addition to measuring the total water signal, T_2 relaxation is also assessed at every point via the CPMG NMR

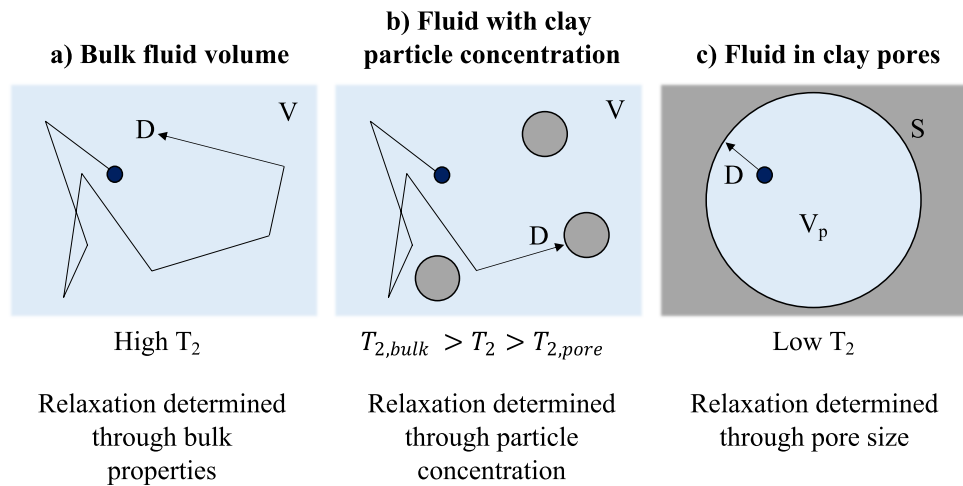
sequence. This relaxation behavior can be influenced by relaxation centers, such as clay particles, which is schematically given in Fig. 4. In the case of free water, see Fig. 4a, there are no relaxation centers, resulting in long bulk relaxation time of water itself, i.e., for free water $T_1 = T_2 = 3$ s. For a system containing clay particles, we must distinguish between two scenarios: a suspension containing free-floating particles (Fig. 4b) or water within a porous structure composed of clay particles, i.e., water within a pore structure (Fig. 4c). In water containing clay particles, the relaxation is related to the concentration of clay particles within the water, whereas for water within a porous clay structure the relaxation is determined by the size of the pores. Within both systems, the water signal decays more quickly than for pure water.

Generally, T_2 relaxation mechanisms in the sediment bed (or other porous media) can be divided in three categories: bulk relaxation, determined by the properties of the bulk fluid; surface relaxation, determined by the interaction between the fluid and clay/solid interface; and diffusion relaxation, related to the dephasing of nuclear spins due to movement through changing magnetic fields (Brownstein and Tarr 1979; Elsayed et al. 2023; Valckenborg et al. 2001a, b). These T_2 contributions of the relaxation mechanisms are given by (Paul Callaghan 1994):

$$\frac{1}{T_2} = \frac{1}{T_{2,v}} + \frac{1}{T_{2,s}} + \frac{1}{T_{2,D}} = \frac{1}{T_2, V} + \rho_2 \frac{S}{V_p} + \frac{1}{12} D(\gamma G TE)^2 \tag{4}$$

where $T_{2,v}$, $T_{2,s}$ and $T_{2,D}$ are the bulk, surface, and diffusion relaxation respectively. ρ_2 is the transverse surface relaxivity due to the susceptibility mismatch of the water and the clay surface. Finally, there is also a contribution due to the diffusion in water in the magnetic gradient of the NMR system. The surface relaxivity can be determined by NMR

Fig. 4 A schematic representation of various T_2 relaxation regimes in clay-water suspensions. D is the diffusion coefficient of water, V_p the pore volume of a pore and S the surface of the pore. Relaxation speed of H-NMR signal is dependent on fluid regime: bulk water with no relaxation centers results in slow signal decay (a); fluids with higher particle concentrations which can act as relaxation center result in faster signal decay (b); fluids confined in pores result in fastest signal decay due to relaxation at the pore walls (c)



CPMG and micro-CT methods or directly from NMR D - T_2 experiments (Benavides et al. 2017, 2020; Luo et al. 2015; Slijkerman and Hofman 1998), hence giving direct access to the pore size.

For fluids in porous media, the bulk relaxation can usually be ignored in the case the pores are small like for clays. Furthermore, if one utilizes short echo time TE or assumes to be in the fast-diffusion regime, the diffusion-based relaxation component is negligible. Assuming that the pores are spherical with radius a gives a volume-to-surface ratio of $\frac{V}{S} = \frac{a}{3}$ (using other geometries will give other ratio's), Eq. (4) can be reduced to:

$$\frac{1}{T_2} \approx \rho_2 \frac{S}{V_p} = \frac{\rho_2^3}{a} \quad (5)$$

This shows that T_2 time can be directly related to the pore size of clay, as shown in Fig. 3c and Fig. 1 in the particle bed. Therefore, by measuring signal decay via a CPMG sequence, both water/clay volume fractions as pore size distributions can be determined via Eq. (4) and (6). It should be noted that within these sedimenting systems, pore size distributions may only be calculated within the particle bed, not for the suspension phase or intermediate phase between suspension in bed in which pores are ill-defined.

3 Multi-slice NMR method, stepper motor and frequency

Although the clay/water volume fraction and pore size distribution can be measured simultaneously and nondestructively via Eqs. (4) and (6), challenges remain related to the acquisition time of a profile via NMR. As mentioned in Sect. 2.1, the T_1 time of hydrogen in water limits the spatio-temporal resolution that can be achieved, specifically affecting the long-delay/repetition time (TR) of a single-slice NMR

measurement. This limitation is schematically represented in Fig. 4a. Only one NMR experiment can be performed every $4T_1$ in a single-slice NMR algorithm, making single-slice NMR techniques rather slow. In cases of sedimentation, the process is fully determined by the slowest relaxation, i.e., by water ($T_1 \approx 3$ s) meaning an NMR experiment can only be repeated every $4T_1$ (~ 12 s), rendering the NMR measurement too slow to observe the initial sedimentation process. To speed up acquisition time of NMR experiments involving water, commonly contrast agents such as CuSO_4 are added to shorten the T_1 time of water. As these chemical contrast agents might affect the sedimentation process of clayey soils however, no contrast fluids can be added to the suspensions.

To accelerate acquisition time and prevent artifacts, we instead introduce a multi-slice method, based on a stepper motor, illustrated in Fig. 5b. Instead of waiting for $4T_1$ between measurements, a second NMR experiment can be initiated by moving to another non-excited position in the sample. In principle, multiple slices can be excited within one acquisition time of $4T_1$, i.e., roughly every T_1 , reducing the measurement time for a profile by a factor of four in this example. To prevent interference from other slices during a single measurement, the measured slices must be properly spaced so that only one slice is present in the sensing coil region of the NMR machine at any given time. This spacing is achieved by using a stepper motor connected to the sample, which moves the sample through the NMR machine in an n-skip-m multi-slice fashion, stopping at specific intervals to carry out measurements. This multi-slice stepper method improves spatial and temporal resolution. This multi-slice stepper method improves spatial and temporal resolution in small-scale 1D NMR systems, which consist of electromagnets generating low static fields (0.78 T) and gradients (± 0.1 T/m), and feature small coils. Moreover by this multi-slice stepper method we overcome the limitations by the long relaxation of water (TR ~ 10 s).

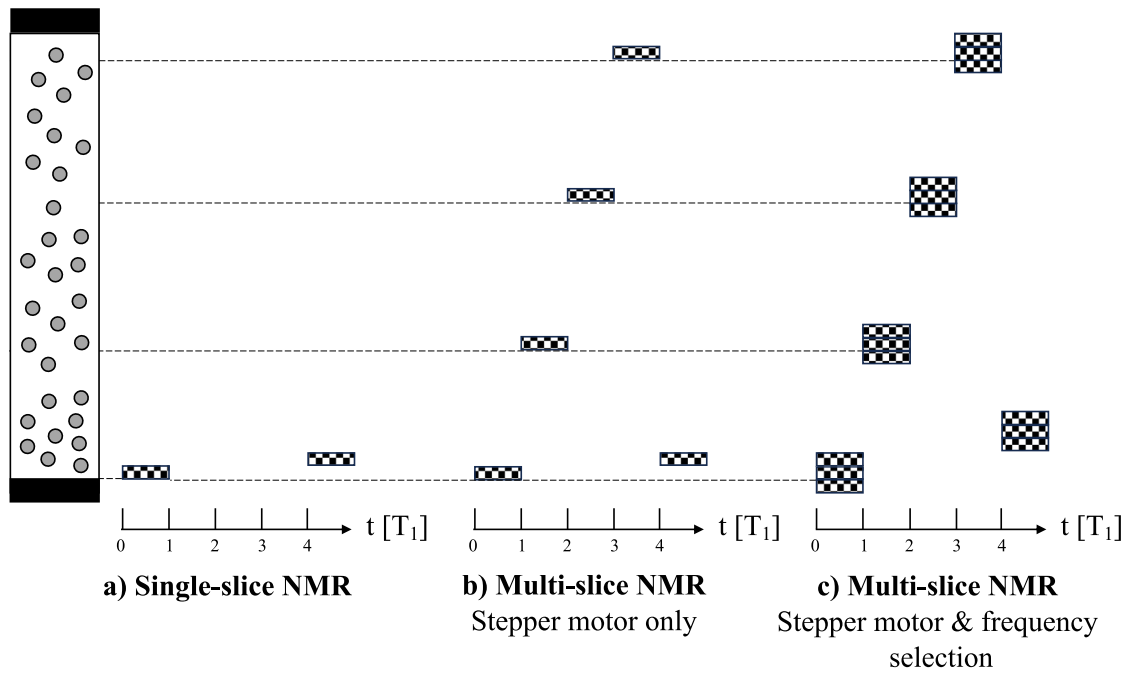


Fig. 5 Schematic representation of various NMR measurement protocols, where measurement periods are given by gray rectangles. By incorporating a stepper motor multi-slice protocol, more measure-

ments can be taken within a single repetition time $TR = 4T_1$. By additionally incorporating frequency-based selection, more datapoints can be acquired per measurement

The multi-slice method via physical stepper motor is supplemented with frequency-based multi-slice encoding, further speeding up acquisition time (Fig. 5c). The frequency-based selection method allows multiple points to be acquired within one measurement by applying a magnetic gradient during the measurement:

$$B_z(z) = B_{z,0} + Gz \tag{6}$$

where $B_{z,0}$ is the homogenous field and G the slice selection gradient. As the Larmor frequency of hydrogen is dependent on the applied field via Eq. (1), one can derive the signal per point z by applying a Fourier transform and using Eq. (7). The frequency-based selection step makes it possible to achieve sub-millimeter spatial resolutions without sacrificing measurement time, while the stepper motor-based method allows fast imaging of large samples that extend beyond the homogenous field of the NMR system, circumventing the single-slice repetition time limit TR .

4 Experimental setup

The NMR setup as used in this study is schematically represented in Fig. 6. The setup consists of a electromagnet (GMW Magnet 3473-70) that provides a magnetic field B_0 of 0.78 T. Quantative NMR measurements are made possible due to Faraday shielding of the high-frequency coils of the

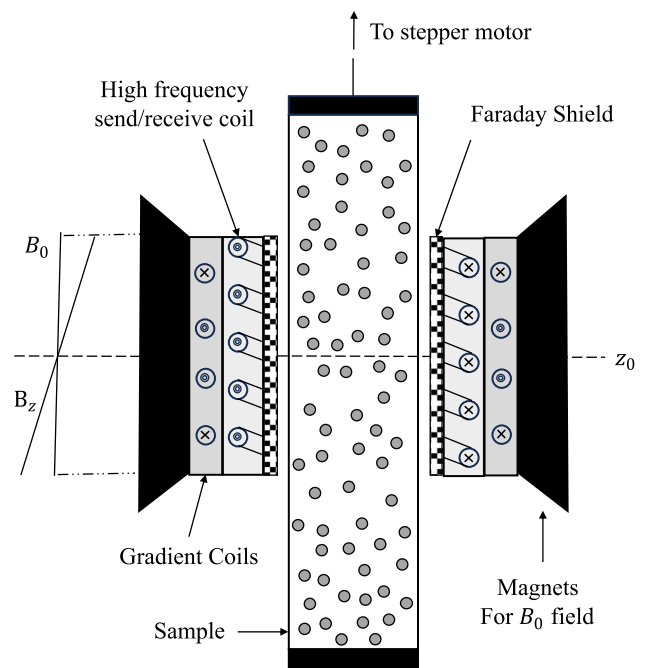


Fig. 6 A diagram of the NMR system for measuring the clay volume fraction and pore size distributions during sedimentation. The main field is applied by an electromagnet generating a field of 0.78 T. Incorporated in the setup is a Faraday shield to prevent detuning of coil due to changing dielectric properties of the volume within the coil. The tube diameter is 23 mm and has a length of 200 mm and can be moved through the NMR machine with the help of a stepper motor with speed ramping algorithm with a maximum acceleration of 3.14 cm/s^2

NMR machine. Without the Faraday shielding, moving samples through the system would change the dielectric properties of the volume contained within the coil and therefore the tuning properties of the LC circuitry of the coil, resulting in a mismatch and signal decline (Conradi and Zens 2019).

In the experiments given in this study, a CPMG sequence of 2048 pulses with $TE = 300\mu s$ at magnetic gradient $G = 0.11T/m$ is used. With the chosen pulse length of $30\mu s$ a slice is excited with a thickness in the order of 3 mm. As the sedimentation of clay sludges is a gravity-influenced phenomenon, the stepper motor uses a speed ramping algorithm with a maximum acceleration of $3.14cm/s^2$ (0.32% of gravity) to limit acceleration-induced disturbances by the stepper-based multi-slice measurement method.

Figure 7 schematically represents the complete control system of the NMR and stepper motor. A central computer system running MATLAB 2021a manages both the stepper motor and the NMR. At the core of the NMR is the SpinCore TRX-I-50-75-300-AW RadioProcessor, an RF acquisition and excitation system with digital detection and real-time signal processing. The RF pulses are amplified by an RF power amplifier to excite the hydrogen spins in the sample. The returning spin-echo signals are pre-amplified and pre-processed by the SpinCore RadioProcessor before being sent to the PC for final data processing in MATLAB, such as calculating the relaxation times.

In this setup, the magnetic gradient is not switched during the CPMG pulse train; it is controlled by the MATLAB script to remain constant and is only switched on and off after an NMR experiment. This approach allows for much shorter spin-echo times, enabling the determination of

relaxation times for smaller pore sizes. Since the gradient is kept constant, only a small region is imaged (~ 3 mm) and a profile over the sample is obtained by moving the sample using the stepper motor. Additionally, a multi-step method is introduced as discussed to limit the scan time for a profile due to the relaxation limitations of water. The stepper motor itself is controlled by an Arduino which runs the software for smooth acceleration and deceleration of the sample.

A single custom MATLAB script controls NMR pulse sequences, sends commands to the stepper motor to move the sample through the NMR, processes signals retrieved from the NMR and performs data analysis. To allow MATLAB to interface with the stepper motor (an RS 440-458 stepper motor), an Arduino Due and Microstepper controller is used. To control the NMR, MATLAB sends commands to a SpinCore TRX-I-50-75-300-AW RadioProcessor. The RadioProcessor serves as a complete NMR system console for generating excitation pulses, sent to the NMR coils high-frequency power amplifiers, and acquiring data from the NMR experiment. The acquired data are then sent to MATLAB for further processing.

5 Results

As a typical example, the sedimentation process of a standard kaolinite suspension is studied using the proposed NMR multi-slice method. A 100 g/l homogenous kaolinite suspension in deionized water is prepared by mixing dry clay powder with deionized water (see Appendix 1 for sample properties). Roughly 80 ml of the suspension is deposited in a

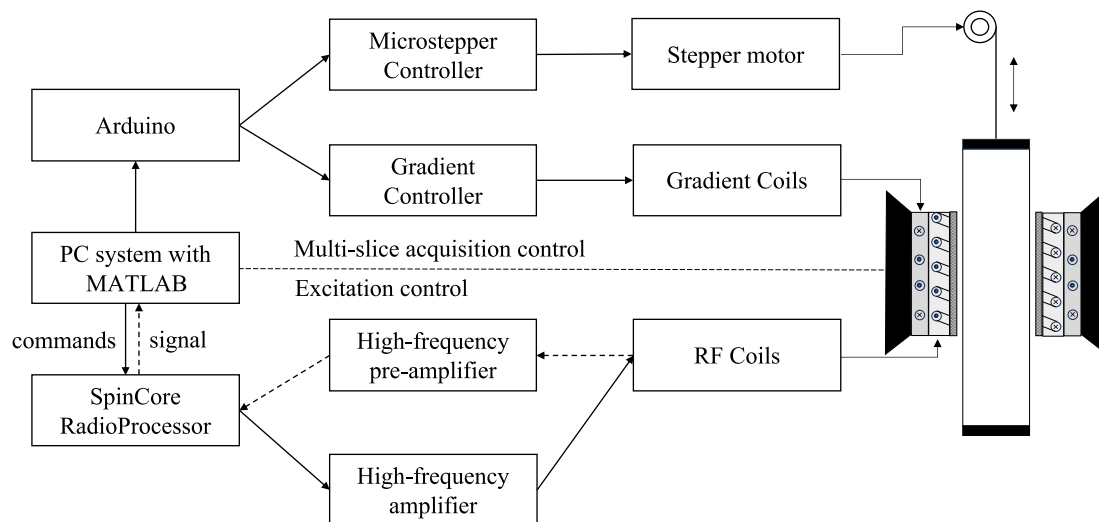


Fig. 7 A schematic diagram of the NMR setup and control of the stepper motor. The high-frequency coils and gradient coils are controlled by a SpinCore RadioProcessor, a digital data acquisition and excitation system, which also processes raw data received by the

NMR system. The specific pulse sequences and pulse parameters are supplied to the SpinCore via MATLAB, running on a PC system connected to the SpinCore. The PC also controls and Arduino, responsible for operating the stepper motor and the gradient controller

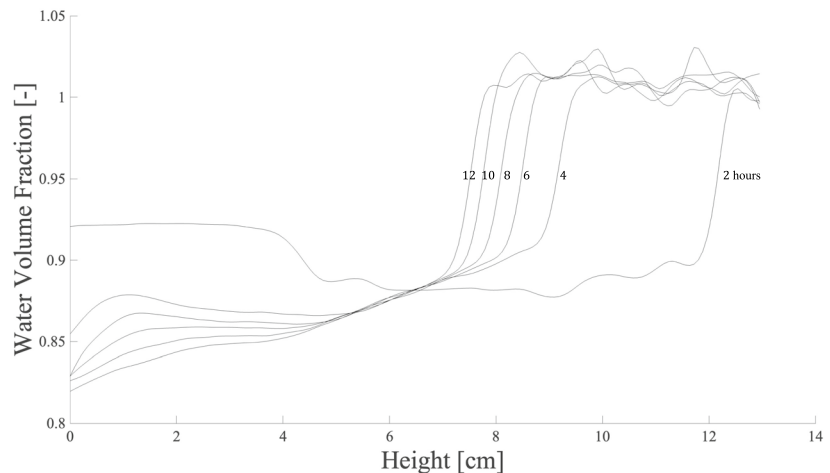
200-mm-high, 23-mm-wide cylindrical glass tube and mixed thoroughly before use. A surface relaxivity of $\rho_2 = 1.8 \mu\text{s}/\text{m}$ is assumed for the kaolinite sample (Elsayed et al. 2023).

To show the effect of the required acquisition time of the NMR method, the single-slice NMR method (Fig. 5a) is compared to the multi-slice stepper with frequency selection method (Fig. 5c). The result for the first 12 h of sedimentation is shown in Fig. 8. Measurements are spaced roughly every two hours. As the clay sample is shaken before the measurement, the clay concentration should be homogenous at the start. While the single-slice method shows artifacts (Fig. 8a), especially in the pure water regime (noisy data) and during the first parts of the sedimentation process (skewed profiles), the multi-slice method accurately determines the sedimentation process. This can be mainly attributed to the decrease in acquisition time, going from 100 min at 0.8 mm resolution using

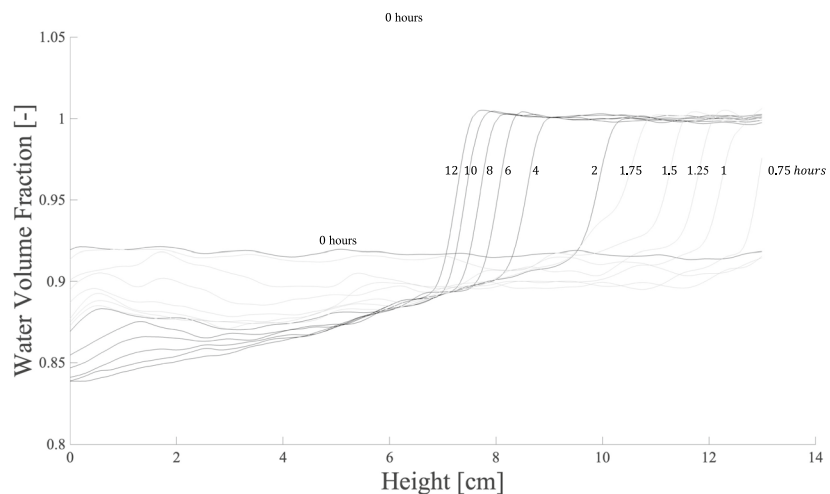
the single-slice method to 12 min at 0.6 mm resolution using the multi-slice method. Due to the almost tenfold increase in measurement speed, more profiles can be acquired. These additional profiles (included in Fig. 8b as gray lines) provide more information on the initial process giving direct access to the sedimentation dynamics.

In Fig. 9, a typical measurement of the kaolinite sedimentation process within the first 36 h is given, where a profile measurement is started every 15 min using the combined multi-slice NMR method. One NMR measurement is carried out per slice (no averaging methods are used). To reduce effects related to noise, data are fitted to a 2D cubic spline using MATLAB, interpolating on a fixed time/space grid, reducing the noise. Information on both volume fractions and pore size distributions in the particle bed is given over time and space.

Fig. 8 Comparison of water volume profile derived from the single-slice NMR algorithm and the combined multi-slice NMR algorithm with a 100 g/l clay suspension in deionized water during the first 12 h of sedimentation (profiles as black lines). Due to increased acquisition speed, additional profiles are acquired during the first two hours of sedimentation using the multi-slice algorithm (light gray lines)



a) Single slice NMR algorithm



b) Multi-Slice combined NMR algorithm

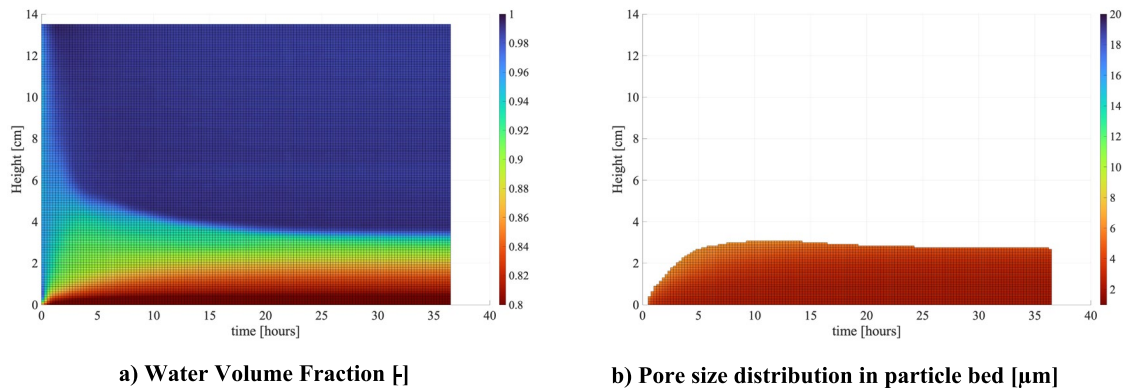


Fig. 9 **a** Sedimentation profiles of kaolinite clay in deionized water over time in volume fraction of water ϕ_{water} measured every quarter hour; **b** derived pore size distribution profiles over time of kaolinite via Eq. (6)

Using this NMR method, both the initial hindered settling and the consolidation phases can be quantitatively measured, as can be seen in Fig. 9a, where we have given the volume fraction as function of time and space. A clear distinction can be seen between the interfaces of the different phases: the suspension phase (predominant during the first half hour), the soft sediment layer at the bottom of the sample (growing over time) and the clear water phase at the top (increasing over time).

As at every position in time, the T_2 relaxation is measured besides the water volume fraction, the pore size distribution can be derived using Eq. (6) as function of the height in the particle bed (see Fig. 9b). As kaolinite clay has one dominant pore size, a mono-exponential decay model was used to fit the relaxation data (Valckenborg et al. 2001a, b). As the sediment layer builds up over time, we observe a pore size change a function of the height in the particle bed, i.e., there are smaller pores formed at the bottom as the consolidated clay layer compacts under the influence of gravity. Hence using NMR, we can see the pore size changing as in time the system is compacting.

6 Conclusions

Using NMR can get a direct insight into the dynamic processes of the sedimentation and consolidation of clay suspensions. The proposed multi-slice NMR method, making use of a physical stepper motor and frequency-based selection, results in a tenfold increase in measurement speed as opposed to traditional single-slice NMR methods. Using this method, a full profile could be measured in 12 min

at a resolution of 0.6 mm, providing information on both pore size distributions within the clay particle bed, as well as water/clay volume fractions in the total sedimentation column over time. This measurement time is short enough (around 10 min) to also measure on the dynamic initial sedimentation. Moreover, the proposed method is suitable for use in low-field NMR scanners (0.78 T) with small homogenous magnetic fields (on the order of millimeters) and hence suitable to also measure on slower sedimentation over a longer time.

While in this paper the T_2 relaxation was used to determine the pore size distribution, the T_2 signal could also be used to derive the clay particle in diluted water mixtures, which we will incorporate in our future research, hence providing the complete information on the sedimentation and consolidation process of clay suspensions.

Appendix

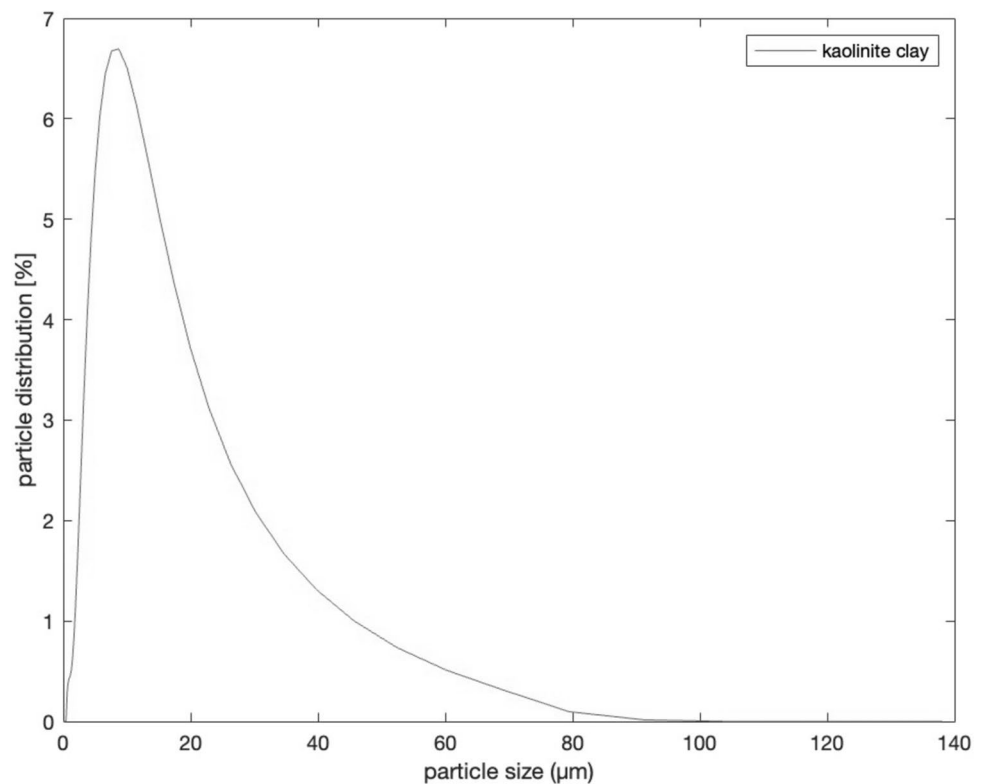
1 Kaolinite sample properties

See Table 1 and Fig. 10.

Table 1 Properties of used 200 g l kaolinite suspension

Parameter	Value
D10–D50–D90 [μm]	1.98–6.18–22.33
pH	9.0
Conductivity [m S/cm]	0.163
Zeta potential [mV]	–24.61

Fig. 10 Particle size distribution of used kaolinite clay suspension



Acknowledgements The authors would like to acknowledge Ismail Myouri (TU Delft, Netherlands) for helpful discussions on the topic of clay sedimentation and for the preparation of the samples used in this study. The authors would also like to the TU Delft MUDNET community for the overall support and sparring sessions made during the project.

Authors contributions Nick J. Hol (N.H.) developed the experimental procedure and parameters, performed experimental measurements, developed the back-end NMR code and data post-processing algorithms, prepared data for analysis and executed data analysis. Leo Pel (L.P.) developed experimental procedure and parameters. Martijn Kurvers (M.K.) built the experimental NMR setup and developed back-end NMR code. Claire Chassagne (C.C.) prepared experimental samples and provided feedback on data analysis. N.H. wrote the first draft. N.H., L.P and C.C. contributed to manuscript editing and review prior to submission.

Funding This project has been made possible partly due to the the Sediment to Soil project (S2S): NWO Open technology program grant 2020-II TTW ref. 13314.

Data availability NMR Sedimentation Data can be made available upon request to the corresponding author.

Declarations

Conflict of interest The authors declare no competing interests.

Ethical approval Not applicable.

References

- Been K, Sills GC (1981) Self-weight consolidation of soft soils: an experimental and theoretical study. *Geotechnique* 31(4):519–535. <https://doi.org/10.1680/GEOT.1981.31.4.519>
- Benavides F, Leiderman R, Souza A, Carneiro G, Bagueira R (2017) Estimating the surface relaxivity as a function of pore size from NMR T2 distributions and micro-tomographic images. *Comput Geosci* 106:200–208. <https://doi.org/10.1016/J.CAGEO.2017.06.016>
- Benavides F, Leiderman R, Souza A, Carneiro G, de Vasconcellos B, Azeredo R (2020) Pore size distribution from NMR and image based methods: a comparative study. *J Petrol Sci Eng* 184:106321. <https://doi.org/10.1016/J.PETROL.2019.106321>
- Brownstein KR, Tarr CE (1979) Importance of classical diffusion in NMR studies of water in biological cells. *Phys Rev A* 19(6):2446. <https://doi.org/10.1103/PhysRevA.19.2446>
- Callaghan P (1994) Principles of nuclear magnetic resonance microscopy, 1st edn. Oxford Science Publications
- Carr HY, Purcell EM (1954) Effects of diffusion on free precession in nuclear magnetic resonance experiments. *Phys Rev* 94(3):630. <https://doi.org/10.1103/PhysRev.94.630>
- Chassagne C (2021) Introduction to colloid science: applications to sediment characterization. In: TU Delft OPEN Books. <https://doi.org/10.34641/MG.16>
- Conradi MS, Zens AP (2019) RF shielding and eddy currents in NMR probes. *J Magn Reson* 305:180–184. <https://doi.org/10.1016/J.JMR.2019.06.011>
- Elsayed M, El-Husseiny A, Hussaini SR, Mahmoud M (2023) Experimental and simulation study on the estimation of surface relaxivity of clay minerals. *Geoenergy Sci Eng* 230:212260. <https://doi.org/10.1016/J.GEOEN.2023.212260>

- Fleury M, Gautier S, Norrant F, Kohler E (2011) Characterization of nanoporous systems with low field NMR: application to kaolinite and smectite clays
- Fouinat L, Sabatier P, Poulenard J, Reyss J-L, Montet X, Arnaud F (2017) A new CT scan methodology to characterize small aggregation gravel clast contained in soft sediment matrix. *Earth Surf Dyn* 5(1):199–209
- Hornak JP (1996) The basics of NMR. Rochester Institute of Technology, Center for Imaging Science
- Imai G (1981) Experimental studies on sedimentation mechanism and sediment formation of clay materials. *Soils Found* 21(1):7–20. <https://doi.org/10.3208/SANDF1972.21.7>
- Komoroski RA (1993) Nonmedical applications of NMR imaging. *Anal Chem* 65(24):1068–1077. <https://doi.org/10.1021/ac00072a714>
- Kresse B, Höfler MV, Privalov AF, Vogel M (2019) One dimensional magnetic resonance microscopy with micrometer resolution in static field gradients. *J Magn Reson* 307:106566. <https://doi.org/10.1016/j.jmr.2019.106566>
- Luo Z-X, Paulsen J, Song Y-Q (2015) Robust determination of surface relaxivity from nuclear magnetic resonance DT 2 measurements. *J Magn Reson*. <https://doi.org/10.1016/j.jmr.2015.08.002>
- Meiboom S, Gill D (1958) Modified spin-echo method for measuring nuclear relaxation times. *Rev Sci Instrum* 29(8):688–691. <https://doi.org/10.1063/1.1716296>
- Merckelbach LM, Kranenburg C (2004) Determining effective stress and permeability equations for soft mud from simple laboratory experiments. *Geotechnique* 54(9):581–591. <https://doi.org/10.1680/GEOT.2004.54.9.581>
- Naghipour N, Ayyoubzadeh S, Sedighkia M (2014) Investigation on the effect of different factors on clay particle sedimentation in freshwaters. *J Biodivers Environ Sci* 5(5):75–81
- Reilly BT, Stoner JS, Wiest J (2017) SedCT: MATLAB™ tools for standardized and quantitative processing of sediment core computed tomography (CT) data collected using a medical CT scanner. *Geochem Geophys Geosyst* 18(8):3231–3240. <https://doi.org/10.1002/2017GC006884>
- Slijkerman WFJ, Hofman JP (1998) Determination of surface relaxivity from NMR diffusion measurements. *Magn Reson Imaging* 16(5–6):541–544. [https://doi.org/10.1016/S0730-725X\(98\)00058-7](https://doi.org/10.1016/S0730-725X(98)00058-7)
- Sutherland BR, Barrett KJ, Gingras MK, Sutherland BR, Barrett KJ, Gingras MK (2015) Clay settling in fresh and salt water. *Environ Fluid Mech* 15:147
- Valckenborg RME, Pel L, Hazrati K, Kopinga K, Marchand J (2001a) Pore water distribution in mortar during drying as determined by NMR. *Mater Struct* 34(10):599–604. <https://doi.org/10.1007/BF02482126>
- Valckenborg RME, Pel L, Kopinga K (2001b) NMR relaxation and diffusion measurements on iron(III)-doped kaolin clay. *J Magn Reson* 151(2):291–297. <https://doi.org/10.1006/JMRE.2001.2384>
- Xuekui W, Qingqing W (2021) Study on sedimentation characteristics of soft clay. In: E3S web of conferences, vol 236, p 02039. <https://doi.org/10.1051/E3SCONF/202123602039>

Springer Nature or its licensor (e.g. a society or other partner) holds exclusive rights to this article under a publishing agreement with the author(s) or other rightsholder(s); author self-archiving of the accepted manuscript version of this article is solely governed by the terms of such publishing agreement and applicable law.

Authors and Affiliations

Nick J. Hol¹ · Leo Pel¹ · Martijn Kurvers¹ · Claire Chassagne²

✉ Leo Pel
l.pel@tue.nl

¹ Transport in Permeable Media, Department of Applied Physics, Eindhoven University of Technology, P.O. Box 513, 5600 MB Eindhoven, The Netherlands

² Environmental Fluid Mechanics, Faculty of Civil Engineering and Geosciences, Delft University of Technology, Box 5048, 2600 GA Delft, The Netherlands